

# Interplay between temperature and trap effects in one-dimensional lattice systems of bosonic particles

Giacomo Ceccarelli, Christian Torrero, Ettore Vicari  
*Dipartimento di Fisica dell'Università di Pisa and I.N.F.N.,  
 Sezione di Pisa, Largo Bruno Pontecorvo 2, I-56127 Pisa, Italy*  
 (Dated: August 4, 2011)

We investigate the interplay of temperature and trap effects in cold particle systems at their quantum critical regime, such as cold bosonic atoms in optical lattices at the transitions between Mott-insulator and superfluid phases. The theoretical framework is provided by the one-dimensional Bose-Hubbard model in the presence of an external trapping potential, and the trap-size scaling theory describing the large trap-size behavior at a quantum critical point. We present numerical results for the low-temperature behavior of the particle density and the density-density correlation function at the Mott transitions, and within the gapless superfluid phase.

PACS numbers: 67.85.-d, 05.30.Rt, 05.30.Jp

Many-body phenomena in dilute atomic gases can be investigated in experiments of cold atoms in optical lattices created by laser-induced standing waves, such as Mott-Hubbard transitions in bosonic gases, see, e.g., Refs. [1–9]. An important feature of these experiments is the presence of a confining potential which traps the particles within a limited spatial region of the optical lattice. The theoretical framework [10] is based on the Bose-Hubbard (BH) model [11]

$$H_{\text{BH}} = -\frac{J}{2} \sum_{\langle ij \rangle} (b_i^\dagger b_j + b_j^\dagger b_i) + \frac{U}{2} \sum_i n_i (n_i - 1) + \mu \sum_i n_i + \sum_i V(r_i) n_i, \quad (1)$$

where  $\langle ij \rangle$  is the set of nearest-neighbor sites, and  $n_i \equiv b_i^\dagger b_i$  is the particle density operator. We assume a power-law space dependence for the external potential which gives rise to the trap, i.e.

$$V(r) = v^p r^p, \quad (2)$$

with even  $p$ . The trap size is defined as

$$l \equiv J^{1/p} / v. \quad (3)$$

Far from the origin the potential  $V(r)$  diverges, therefore  $\langle n_i \rangle$  vanishes and the particles are trapped. Experiments are usually set up with a harmonic potential, i.e.  $p = 2$ . In the following we set  $J = 1$ , so that  $l = 1/v$ .

The homogeneous BH model without trap undergoes continuous quantum transitions between superfluid and Mott-insulator phases, driven by the chemical potential  $\mu$ . In one and two dimensions the length scale of the critical modes diverges with the exponent  $\nu = 1/2$  and the low-energy spectrum scales with the dynamic exponent  $z = 2$  [11, 12]. The superfluid phase is gapless; in one-dimensional systems the low-energy modes are described by a two-dimensional conformal field theory.

In the presence of a trapping potential, theoretical and experimental results have shown the coexistence of Mott-insulator and superfluid regions when varying the total

occupancy of the lattice, see, e.g., Refs. [7, 10, 13–22]. However, at fixed trap size, the system does not develop a critical behavior with a diverging length scale [13, 17]. Criticality can be recovered in the limit of large trap size, by simultaneously tuning the chemical potential to the critical values  $\mu_c$  of the homogenous system. This critical regime can be described in the framework of the trap-size scaling (TSS) theory [23, 24]. At a quantum critical point, the large trap-size behavior of the free-energy density of a  $d$ -dimensional trapped particle system is expected to behave as [23, 25]

$$F(\mu, T, l, x) = l^{-\theta(d+z)} \mathcal{F}(\bar{\mu} l^{\theta/\nu}, T l^{\theta z}, x l^{-\theta}), \quad (4)$$

where  $x$  is the distance from the middle of the trap,  $\bar{\mu} \equiv \mu - \mu_c$  and  $\mu_c$  is the critical value of the chemical potential. The trap exponent  $\theta$  at the Mott transitions is given by

$$\theta = \frac{p}{p+2}, \quad (5)$$

which determines how the length scale of the critical modes diverges with increasing trap size, i.e.  $\xi \sim l^\theta$ , at the critical point. Analogously, the particle density correlator,

$$G(x, y) \equiv \langle n_x n_y \rangle_c \equiv \langle n_x n_y \rangle - \langle n_x \rangle \langle n_y \rangle, \quad (6)$$

is expected to scale as

$$G(x, y) = l^{-2d\theta} \mathcal{G}(\bar{\mu} l^{\theta/\nu}, T l^{z\theta}, x/l^\theta, y/l^\theta). \quad (7)$$

Finite-size effects, when the trap is within a finite box of size  $L$ , can be taken into account by adding a further dependence on the scaling variable  $L/l^\theta$  [26].

The TSS of the one-dimensional (1D) BH model has been investigated at zero temperature [25]. TSS can be derived analytically in the low-density regime, at the superfluid-to-vacuum transition, within the spinless fermion representation of the hard-core limit. The trap-size dependence turns out to be more subtle in the other

critical regions, when the corresponding homogenous system has a nonzero filling  $f$ . In the presence of the trapping potential, the expectation value  $N$  of the particle-number operator  $\hat{N} = \sum_x n_x$  is finite, and increases as  $N \sim l$  with increasing the trap size  $l$  keeping  $\mu$  fixed. Thus, since  $[\hat{N}, H_{\text{BH}}] = 0$ , the lowest-energy states at fixed  $\mu$ , and in particular the ground state, change when  $N$  jumps by 1 with increasing  $l$ , giving rise to an infinite number of level crossings [25]. At the Mott transitions with nonzero integer filling, this gives rise to a modulated TSS: the TSS of the observables is still controlled by the trap-size exponent  $\theta$ , but it gets modulated by periodic functions of the trap size, requiring a minor revision of the TSS ansatz (4) and (7). For example, the particle-density correlation function at  $T = 0$  behaves as  $G(0, x) = l^{-2\theta} g(x/l^\theta, \phi)$  where  $\phi$  is a phase-like variable measuring the distance from the closest level crossing. Note that this phenomenon persists in the limit  $p \rightarrow \infty$ , which corresponds to a homogeneous system with open boundary conditions. Modulations of the asymptotic power-law behavior is also found in the gapless superfluid region, with additional multiscaling behaviors.

In this paper we investigate the interplay of temperature and trap effects in the 1D BH model (1) at the transitions between Mott-insulator and superfluid phases. The results are analyzed and discussed in the theoretical TSS framework, which provides an effective description of the critical behaviors in the presence of the trap. In particular, we address the issue whether the modulation phenomenon found at  $\mu < 1$  and  $T = 0$  persists at finite temperature, or it is effectively averaged out due to the fact that the level crossings of the lowest states are expected to give weaker effects at  $T > 0$ . This study is of experimental relevance, because quasi 1D trapped particle systems have been realized in optical lattices, see, e.g., Refs. [1, 4, 5, 9].

We present numerical results for the 1D BH model, obtained by quantum Monte Carlo (QMC) simulations at fixed trap size  $l$ , based on the stochastic series expansion [27, 28]. The main features of the TSS at the Mott transitions are expected to be universal with respect to the on-site coupling  $U$  (provided  $U > 0$ ), including the hard-core (HC) limit  $U \rightarrow \infty$ . Therefore, we consider the 1D HC BH model [29], which is particularly convenient because it restricts the values of the site particle number to  $n_x = 0, 1$ , and it is expected to minimize the corrections to the universal TSS, as verified at  $T = 0$  [30]. In the absence of the trap, the 1D HC BH model has three phases: the empty state for  $\mu > 1$  with  $\langle n_i \rangle = 0$ , which may be seen as a particular  $n = 0$  Mott phase, a gapless superfluid phase for  $|\mu| < 1$ , and a  $n = 1$  Mott phase for  $\mu < -1$ . See, e.g., Ref. [31]. Therefore, there are two quantum transitions at  $\mu = 1$  and  $\mu = -1$ , which share the same critical exponents  $\nu = 1/2$  and  $z = 2$ . We present finite-temperature results for the particle density and the density-density correlator, at the transitions between the Mott and superfluid phases, and within the gapless superfluid phase. Their temperature and trap-

size dependences appear well described by the simplest TSS ansatz, such as that given in Eq. (7). The finite-temperature data do not show evidence of the modulation phenomenon, which appears averaged out, showing only a plain power-law TSS behavior.

The paper is organized as follows. In Sec. I we study the temperature and trap-size dependences in the low-density regime, where we analytically derive the TSS describing temperature and trap effects, and compare it with QMC simulations at  $\mu = 1$ . Sec. II presents QMC results at the  $n = 1$  Mott transition for  $p = 2$  and  $p \rightarrow \infty$ . In Sec. III we investigate the superfluid phase, presenting QMC results at  $\mu = 0$ . In Sec. IV we study the TSS around the spatial point where the particle density rapidly vanishes when  $\mu < 1$ , which shows a peculiar scaling behavior effectively controlled by a linear external potential. Finally, we draw our conclusions in Sec. V. In App. A we provide some details on the QMC simulations.

## I. THE LOW-DENSITY REGIME

In order to determine the temperature and trap-size dependence in the low-density regime of the 1D HC BH model, around  $\mu = 1$ , we consider the free fermion representation which can be derived by a Jordan-Wigner transformation, see, e.g., Ref. [31],

$$H_c = \sum_{ij} c_i^\dagger h_{ij} c_j, \quad (8)$$

$$h_{ij} = \delta_{ij} - \frac{1}{2} \delta_{i,j-1} - \frac{1}{2} \delta_{i,j+1} + [\bar{\mu} + V(x_i)] \delta_{ij},$$

with  $\bar{\mu} \equiv \mu - 1$ . In the fermion representation the Hamiltonian can be easily diagonalized by introducing new canonical fermionic variables  $\eta_k = \sum_i \phi_{ki} c_i$ , where  $\phi$  satisfies the equation  $\sum_j h_{ij} \phi_{kj} = \omega_k \phi_{ki}$ , obtaining  $H_c = \sum_k \omega_k \eta_k^\dagger \eta_k$ . The ground state contains all  $\eta$ -fermions with  $\omega_k < 0$ .

A nontrivial TSS limit [23] around  $\mu = 1$  is obtained by introducing the continuum function  $\phi_k(x) \equiv \phi_{kx}$ , the rescaled quantities

$$X = x/l^\theta, \quad \mu_r = \bar{\mu} l^{2\theta}, \quad \Omega_k = \omega_k l^{2\theta}, \quad (9)$$

where  $\theta$  is the trap exponent, cf. Eq. (5), and neglecting terms which are suppressed in the large- $l$  limit. This leads to the Schrödinger-like equation

$$\left( -\frac{1}{2} \frac{d^2}{dX^2} + X^p \right) \varphi_k(X) = e_k \varphi_k(X), \quad (10)$$

where  $e_k \equiv \Omega_k - \mu_r$  and  $\varphi_k(X) \equiv \phi_k(l^\theta X)$ .

In the case of a harmonic potential, i.e.  $p = 2$ , we have  $\theta = 1/2$ , and

$$e_k \equiv \Omega_k - \mu_r = 2^{1/2} (k + 1/2), \quad k \geq 0, \quad (11)$$

$$\varphi_k(X) = \frac{2^{1/8} H_k(2^{1/4} X)}{\pi^{1/4} 2^{k/2} (k!)^{1/2}} \exp(-X^2/\sqrt{2}),$$

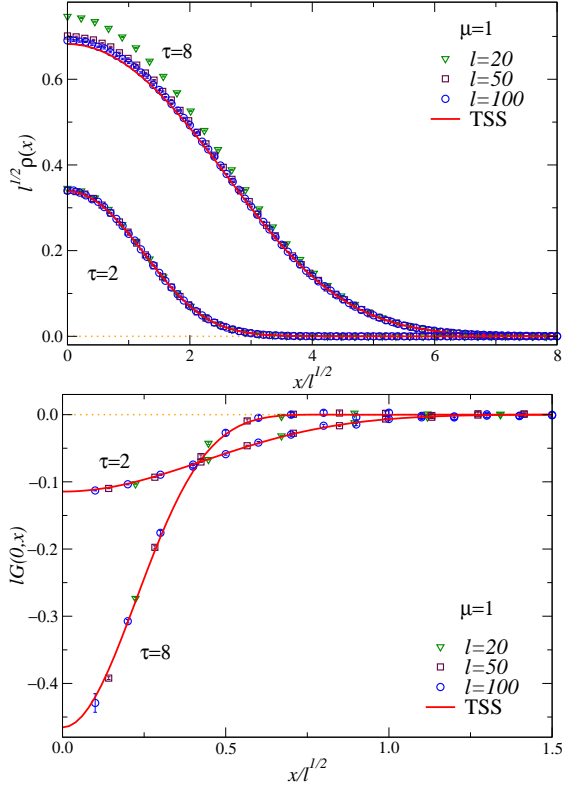


FIG. 1: (Color online) The particle density (top) and the density-density correlator (bottom) in the presence of a harmonic potential, at  $\mu = 1$  and for some values of the trap size  $l$ , at  $\tau \equiv Tl = 8$  and  $\tau = 2$ . The full lines show the TSS functions given by Eqs. (18) and (20).

where  $H_k(x)$  are Hermite's polynomials. For  $p \rightarrow \infty$ , Eq. (10) becomes equivalent to the Schrödinger equation of a free particle in a box of size  $L = 2l$  with boundary conditions  $\varphi(-1) = \varphi(1) = 0$ , thus  $\theta = 1$  and

$$e_k = \frac{\pi^2}{8}(k+1)^2, \quad k \geq 0, \quad (12)$$

$$\varphi_k(X) = \sin \left[ \frac{\pi}{2}(k+1)(X+1) \right].$$

Since

$$n_x \equiv b_x^\dagger b_x = c_x^\dagger c_x, \quad (13)$$

the particle density of bosons and its correlation function (6) are equal to those of the fermions in the quadratic Hamiltonian (8). The fermion two-point function is given by

$$\langle c_x^\dagger c_y \rangle = \sum_{ab} \phi_{ax} \phi_{by} \langle \eta_a^\dagger \eta_b \rangle = \sum_{k=0}^{\infty} \frac{\phi_{kx} \phi_{ky}}{1 + \exp(\omega_k/T)}. \quad (14)$$

Its TSS limit can be written in terms of the eigensolutions of the Schrödinger-like equation (10), as

$$\langle c_x^\dagger c_y \rangle = l^{-\theta} \sum_{k=0}^{\infty} \frac{\varphi_k(X) \varphi_k(Y)}{1 + \exp[(e_k + \mu_r)/\tau]}, \quad (15)$$

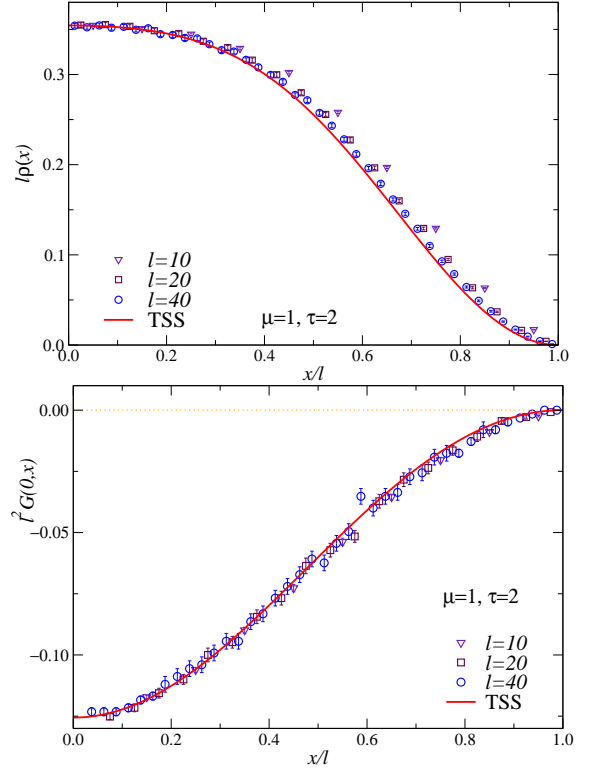


FIG. 2: (Color online) Results for the particle density (top) and the density-density correlator (bottom) at  $\mu = 1$  and  $p \rightarrow \infty$ , for some values of  $l$ , keeping  $\tau \equiv Tl^2 = 2$  fixed. The full line shows the TSS functions given by Eqs. (18) and (20).

where we have introduced the scaling variable

$$\tau \equiv Tl^{2\theta} = Tl^{2\theta}. \quad (16)$$

Then, straightforward calculations allow us to extend the  $T = 0$  results of Ref. [25], to allow for the temperature. We obtain

$$\rho(x) \equiv \langle n_x \rangle = l^{-\theta} \mathcal{D}(\bar{\mu}l^{2\theta}, Tl^{2\theta}, x/l^\theta), \quad (17)$$

$$\mathcal{D}(\mu_r, \tau, X) = \sum_{k=0}^{\infty} \frac{\varphi_k(X)^2}{1 + \exp[(e_k + \mu_r)/\tau]}, \quad (18)$$

and

$$G(x, y) = l^{-2\theta} \mathcal{G}(\bar{\mu}l^{2\theta}, Tl^{2\theta}, x/l^\theta, y/l^\theta), \quad (19)$$

$$\mathcal{G}(\mu_r, \tau, X, Y) = - \left[ \sum_{k=0}^{\infty} \frac{\varphi_k(X) \varphi_k(Y)}{1 + \exp[(e_k + \mu_r)/\tau]} \right]^2, \quad (20)$$

which holds for  $x \neq y$ . Note that  $G(x, y) < 0$  for  $x \neq y$ , but  $G(x, x) \equiv \langle n_x^2 \rangle - \langle n_x \rangle^2 > 0$ , indeed  $\sum_{xy} G(x, y) > 0$ . The above scaling functions describe the asymptotic large trap-size behavior; corrections are suppressed by a further  $l^{2\theta}$  power. Practically exact results for the TSS functions of the harmonic potential and the hard-wall limit, for any  $\mu_r$  and  $\tau$ , can be easily obtained using Eqs. (11) and (12), because the series are rapidly converging.

In Fig. 1 we show QMC results for the harmonic potential at  $\mu = 1$ , for some values of the trap size, keeping  $\tau \equiv Tl$  fixed at  $\tau = 2$  and  $\tau = 8$ . They clearly appear to approach the TSS given by Eqs. (18) and (20). Analogous results are obtained for the hard-wall limit, which is equivalent to a homogeneous system of size  $L = 2l$  with open boundary conditions. Since  $\theta = 1$  in this case, TSS requires keeping  $\tau \equiv Tl^2$  fixed. Results for  $\tau = 2$  are shown in Fig. 2.

The TSS functions in the low-density regime are expected to be universal with respect to the on-site coupling  $U$ , provided that  $U > 0$ . As shown by the calculations at  $T = 0$  reported in Ref. [30], finite values of  $U$  give rise to  $O(l^{-\theta})$  corrections, which decay more slowly than the  $O(l^{-2\theta})$  leading corrections in the HC limit.

## II. TSS AT THE $n = 1$ MOTT TRANSITION

We recall that the quantum critical behavior around  $\mu = -1$  of the homogeneous HC BH model without trap is essentially analogous to that at  $\mu = 1$ , because of the invariance under the particle-hole exchange. At the  $n = 1$  Mott-insulator to superfluid quantum transition, the critical exponents  $\nu$  and  $z$  and the trap-size exponent  $\theta$  are the same as those at  $\mu = 1$ . However, the particle-hole symmetry does not hold in the presence of the trapping potential, and the asymptotic trap-size dependence at  $T = 0$  appears more complicated at the  $n = 1$  Mott transition [25].

In the 1D HC BH model with a trapping potential and  $\mu < 1$ , the ground-state particle density turns out to approach its local density approximation (LDA) in the large- $l$  limit, with corrections that are suppressed by powers of the trap size and present a nontrivial TSS behaviour [25], see also below. Within the LDA, the particle density at the spatial coordinate  $x$  equals the particle density of the homogeneous system at the effective chemical potential

$$\mu_{\text{eff}}(x) \equiv \mu + (x/l)^p. \quad (21)$$

The LDA of the particle density reads  $\langle n_x \rangle_{\text{lda}} \equiv \rho_{\text{lda}}(x/l)$ , where

$$\rho_{\text{lda}}(x/l) = \begin{cases} 0 & \text{for } \mu_{\text{eff}}(x) > 1, \\ (1/\pi) \arccos \mu_{\text{eff}}(x) & \text{for } -1 \leq \mu_{\text{eff}}(x) \leq 1, \\ 1 & \text{for } \mu_{\text{eff}}(x) < -1. \end{cases} \quad (22)$$

The *thermodynamic* limit at fixed  $\mu$  corresponds to the limit  $N, l \rightarrow \infty$  keeping the ratio  $N/l$  fixed. At  $T = 0$  we have

$$N \equiv \left\langle \sum_i b_i^\dagger b_i \right\rangle = \tilde{\rho}(\mu)l + O(1), \quad (23)$$

where  $\tilde{\rho}(\mu) = 2 \int_0^\infty \rho_{\text{lda}}(y) dy$ . Eq. (23) provides the correspondence between the ratio  $N/l$  and  $\mu$  at  $T = 0$ . In

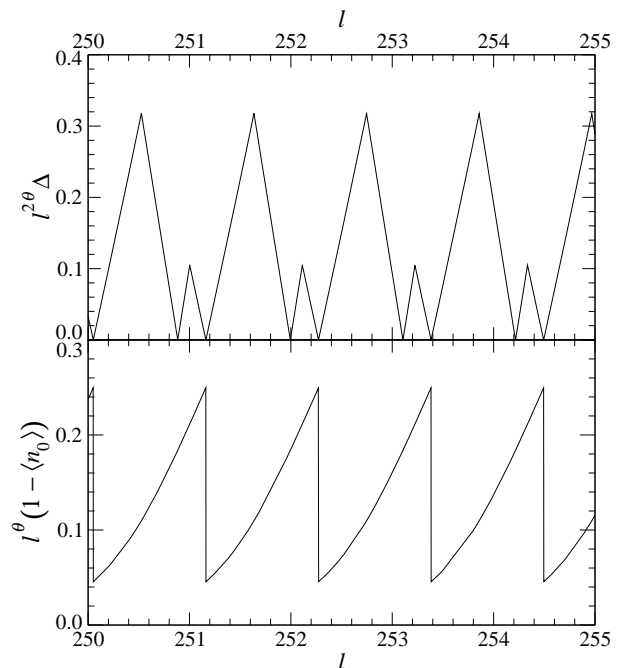


FIG. 3: (Color online) The rescaled difference of the lowest energy levels  $l^{2\theta} \Delta$  (above) and the rescaled particle density  $l^\theta (1 - \langle n_0 \rangle)$  (below) at the center of the trap vs.  $l$  in the middle of the trap for  $p = 2$  and at  $\mu = -1$ .

particular, when  $0 < N/l < \tilde{\rho}(-1)$  the system is essentially in the superfluid phase, while for  $N/l > \tilde{\rho}(-1)$  the  $n = 1$  Mott phase appears around the center of the trap.

The  $T = 0$  trap-size dependence around  $\mu = -1$  is characterized by an infinite number of level crossings of the two lowest energy states, at  $l_0^{(k)}$  with  $k = 1, 2, 3, \dots$  and  $l_0^{(k+1)} > l_0^{(k)}$ . As suggested by Fig. 3, the rescaled energy difference  $l^{2\theta} \Delta$  of the two lowest states shows a periodic structure asymptotically for large  $l$ , as a function of  $l$  [25]. In particular, in the case of a trap centered at the middle site of the lattice and in the large- $l$  limit, the interval

$$P_l \equiv l_0^{(2k+2)} - l_0^{(2k)}, \quad (24)$$

between two even zeroes of such difference approaches a constant value,  $P_l^* \cong 1.11072073$  for  $p = 2$  and  $P_l^* = 1$  for  $p \rightarrow \infty$ . This gives rise to a peculiar modulation of the amplitudes of the power-law behaviors of the observables. For example, the density at the center of the trap behaves as

$$\langle n_0 \rangle - 1 \approx l^{-\theta} f_0(\phi), \quad (25)$$

where  $\phi$  is the phase-like variable

$$\phi = \frac{l - l_0^{(2k)}}{l_0^{(2k+2)} - l_0^{(2k)}}, \quad l_0^{(2k)} \leq l < l_0^{(2k+2)}, \quad (26)$$

which measures the distance from the closest even level crossing. Thus, the amplitudes of the power laws predicted by the TSS show a periodic modulation, see

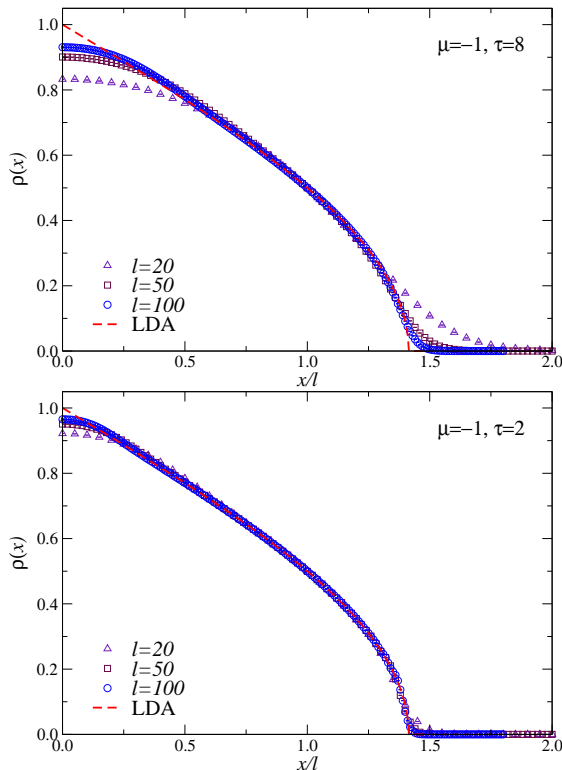


FIG. 4: (Color online) The particle density at  $\mu = -1$  for  $\tau \equiv Tl = 8$  (top) and  $\tau = 2$  (bottom). The full lines represent the LDA approximation (22).

Ref. [25] for details. Moreover, the spatial dependence of the particle density and its correlator turns out to be described by the following scaling behavior at large trap size

$$\rho(x) \equiv \langle n_x \rangle \approx \rho_{\text{lda}}(x/l) + l^{-\theta} f(X, \phi), \quad (27)$$

where  $X = x/l^\theta$ , and

$$G(0, x) \equiv \langle n_0 n_x \rangle_c = l^{-2\theta} g(X, \phi). \quad (28)$$

An interesting question is whether this scenario persists at finite temperature, where the effects of the level crossings of the lowest states are expected to be weaker.

We investigate this issue by comparing QMC data at various increasing values of the trap size keeping fixed the scaling quantity  $\tau = Tl$ . Fig. 4 shows results for the particle density, which appears to approach the LDA approximation (22) with increasing  $l$ , for  $\tau = 2$  and  $\tau = 8$ . This should not be surprising, given that the LDA approximation is asymptotically approached at  $T = 0$ , and the TSS is performed by rescaling  $T$  as  $T = \tau/l$ . Fig. 5 shows the scaling of the subtracted particle density

$$\Delta\rho(x) \equiv \rho(x) - \rho_{\text{lda}}(x/l). \quad (29)$$

Its behavior around the trap appears to behave as

$$\Delta\rho(x) \approx l^{-\theta} \mathcal{D}(X, \tau), \quad (30)$$

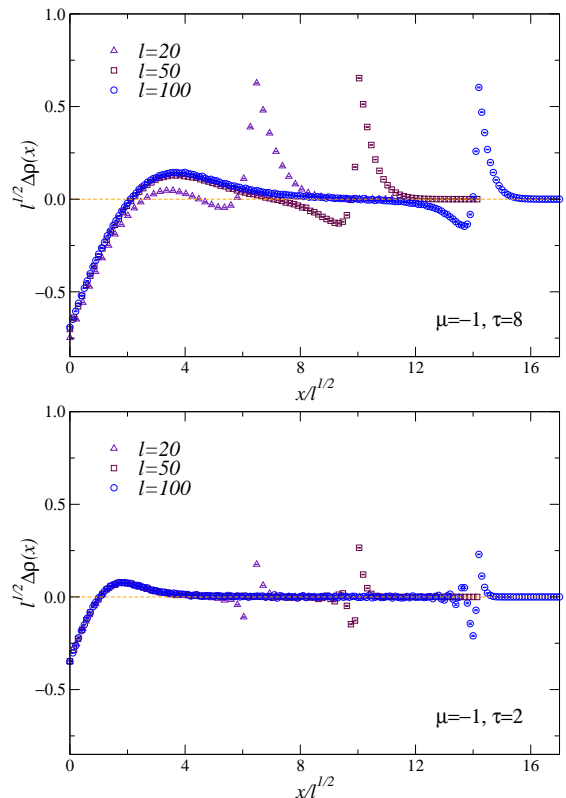


FIG. 5: (Color online) Scaling of the subtracted particle density at  $\mu = -1$  for  $\tau = 8$  (top) and  $\tau = 2$  (bottom).

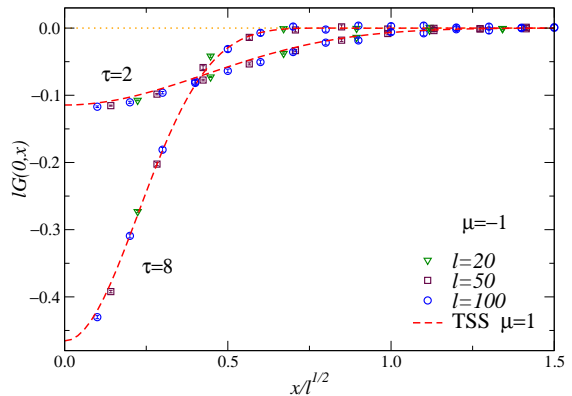


FIG. 6: (Color online) The density correlation at  $\mu = -1$  for values of the trap size  $l$ , at  $\tau \equiv Tl = 8$  and  $\tau = 2$ . The dashed lines show the TSS at  $\mu = 1$ .

without evidences of modulations. Strong deviations from scaling are observed at large distance from the center of the trap, in a region corresponding to  $x \approx \sqrt{2}l$ , which disappears in the TSS limit, because it moves away with increasing  $l$  when the data are plotted versus the rescaled distance  $X \equiv x/l^\theta$  with  $\theta < 1$ . As we shall see in Sec. IV, the behavior around  $x \approx \sqrt{2}$ , where  $\mu_{\text{eff}}(x) \approx 1$ , shows another scaling behavior, effectively controlled by an external linear potential.

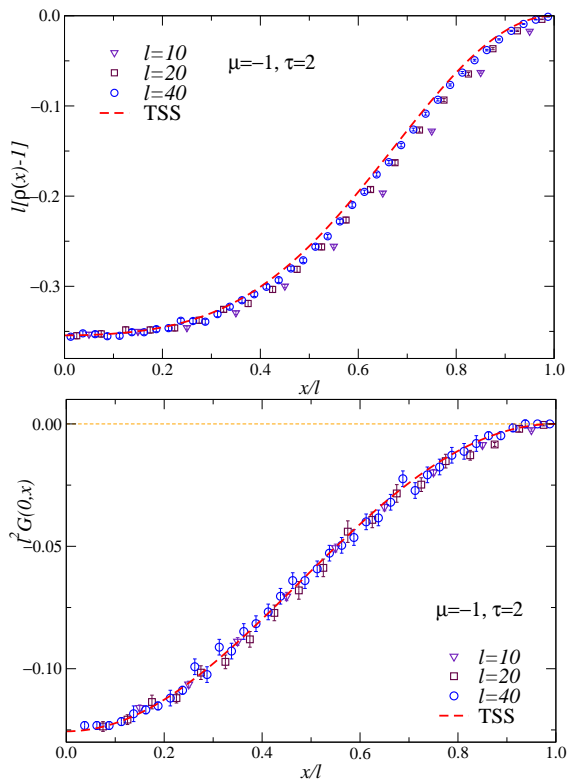


FIG. 7: (Color online) Plots of  $l[\rho(x) - 1]$  (top) and  $l^2 G(0, x)$  (bottom) for  $p \rightarrow \infty$ , at  $\mu = -1$  and  $\tau \equiv Tl^2 = 2$ . The dashed lines show the TSS at  $\mu = 1$ .

Some results for the particle-density correlation  $G(0, x)$ , between the center of the trap and the point  $x$ , are reported in Fig. 6. They show a nice scaling compatible with

$$G(0, x) = l^{-1} \mathcal{G}(X, \tau), \quad (31)$$

again without evidence of modulations. Interestingly, the data appear to approach the same TSS curves found at  $\mu = 1$  for the same values of  $\tau = Tl$ , providing an evidence of universality between the TSS at the  $n = 0$  and  $n = 1$  Mott transitions, at least for the connected correlation functions. Analogous results are found in the limit  $p \rightarrow \infty$ , as shown by the data reported in Fig. 7.

We conclude noting that the apparent absence of modulations indicate that the temperature averages out these effects, so that the temperature and trap-size dependences are well described by the TSS ansatz (4) and (7), in analogy with the low-density regime. Of course, the modulation phenomenon must be somehow recovered in the limit  $\tau \rightarrow 0$ .

### III. TSS WITHIN THE SUPERFLUID PHASE

We now analyze the trap-size dependence within the gapless superfluid phase, whose corresponding continuum

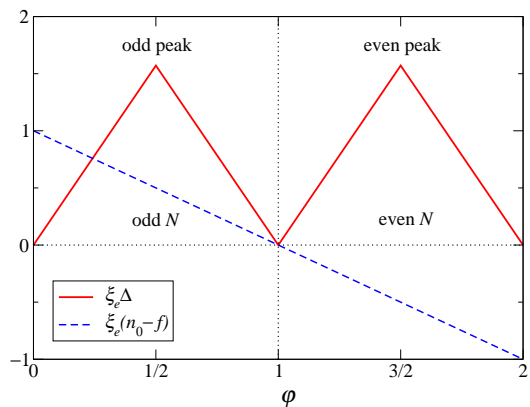


FIG. 8: The asymptotic behaviour of the difference between the lowest-energy states  $\Delta$  and the particle density  $\langle n_0 \rangle$  at the center of the trap at  $\mu = 0$ , thus  $f = 1/2$ , and  $T = 0$ . In formulae  $\Delta = \pi t(\varphi)/\xi_e$  and  $\langle n_0 \rangle = (1 - \varphi)/\xi_e$ , where  $\xi_e \sim l^{-1}$  is the entanglement length scale. These results apply for any  $p$ , including  $p \rightarrow \infty$ . See Refs. [25, 32] for details.

theory is a conformal field theory with  $z = 1$ . The trap-size dependence at zero temperature was investigated in Refs. [25, 32]. Its asymptotic behavior turns out to be characterized by two length scales with different power-law divergence in the large trap-size limit. One of them scales as  $\xi \sim l$  and describes the behavior of observables related to smooth modes, such as the half-lattice entanglement; the other one scales as  $\xi \sim l^\zeta$  with  $\zeta = p/(p+1)$  and it is found in observables involving the modes at the Fermi scale  $k_F = \pi f$ , where  $f$  is the filling of the homogeneous system. Moreover, the asymptotic power law behaviors appear modulated by periodic functions of the trap size, which is again related to level crossings of the two lowest states when increasing the trap size, whose interval

$$Q_l = l_0^{(k+1)} - l_0^{(k)}, \quad (32)$$

tends to a constant:  $Q_l^* = 1.3110287$  for  $p = 2$ , and  $Q_l^* = 1$  for  $p = \infty$ . Indeed, the difference between the two lowest states behaves asymptotically as  $\Delta \sim t(\varphi)l^{-1}$ , where  $\varphi$  is defined as

$$\varphi = 2 \frac{l - l_0^{(2k)}}{l_0^{(2k+2)} - l_0^{(2k)}}, \quad l_0^{(2k)} \leq l < l_0^{(2k+2)}, \quad (33)$$

and  $t(\varphi)$  is a triangle function shown in Fig. 8 where results for  $\mu = 0$  are reported.

At  $T = 0$ , the particle density and its correlation function show a quite complicated behavior [25]. Indeed,

$$\langle n_x \rangle \approx \rho_{\text{lda}}(X) + l^{-1} \Re \left\{ h(Y, \varphi) e^{2ik_F x} + g(Y, \varphi) \right\},$$

$$X = x/l, \quad Y = xl^{-p/(p+1)}, \quad (34)$$

and

$$G_n(x, 0) \approx l^{-2p/(p+1)} \Re \left\{ \tilde{h}(Y, \varphi) e^{2ik_F x} + \tilde{g}(Y, \varphi) \right\}, \quad (35)$$

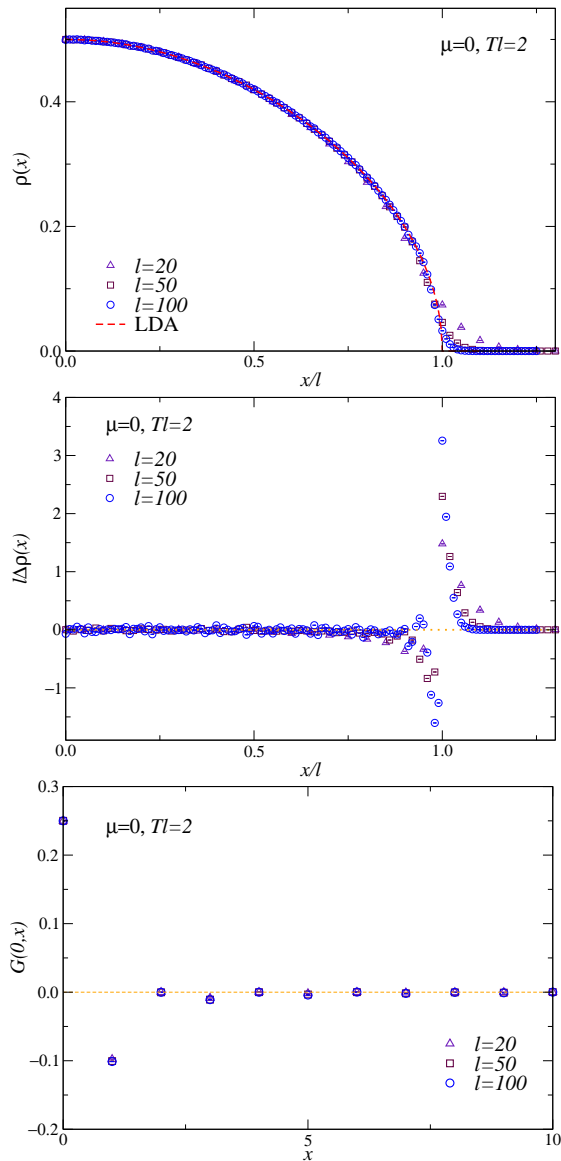


FIG. 9: (Color online) We plot the particle density (top), the rescaled subtracted particle density  $l\Delta\rho$  with  $\Delta\rho \equiv \rho - \rho_{\text{lda}}$  (middle), and the particle density correlator  $G(0, x)$  (bottom) at  $\mu = 0$  and  $T = 2/l$ , in the case of the harmonic potential.

where  $k_F = \pi f = \arccos \mu$ , and terms suppressed by higher powers of  $l^{-1}$  are neglected.

In Fig. 9 we show results for the particle density and various values of the trap size with  $T = 2/l$ . We choose this scaling of the temperature because the trap exponent associated with the smooth modes is expected to be  $\theta = 1$  [25]. The results are clearly converging toward the corresponding LDA approximation. Around the center of the trap, we do not observe the modulated scaling found at  $T = 0$ . Only around  $x \approx l$  we observe some significant differences which decrease with increasing  $l$ , see below. Moreover, the data for the particle-density correlator  $G(0, x)$  appear to vanish after a few lattice spacings for any  $l$ , without showing any particular scaling. There-

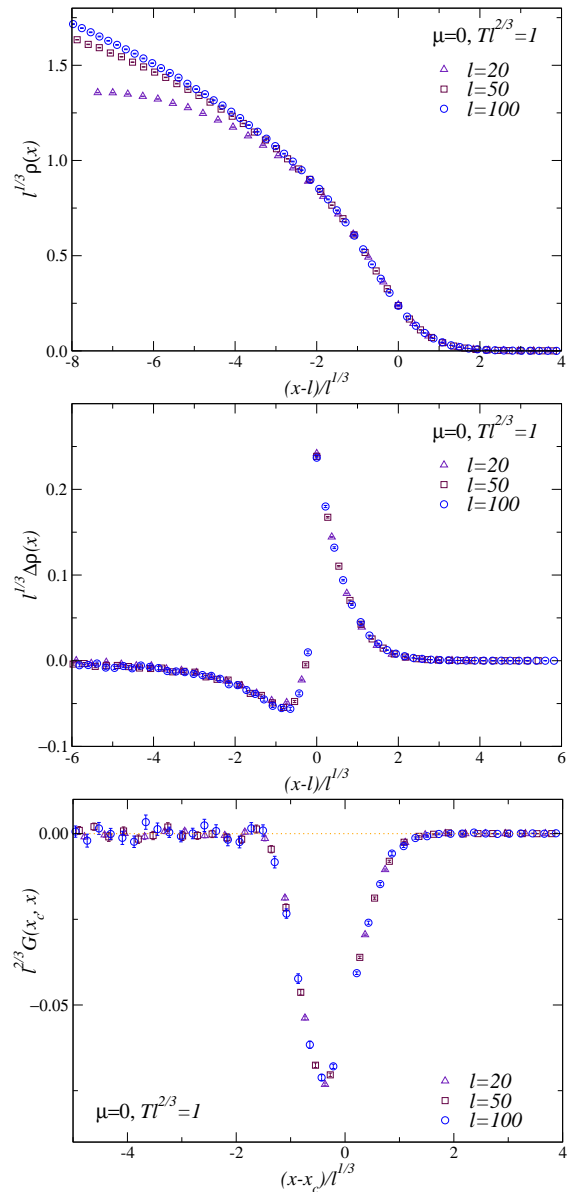


FIG. 10: (Color online) Scaling of the particle density (top), the subtracted particle density  $\Delta\rho \equiv \rho - \rho_{\text{lda}}$  (middle) and the particle density correlator (bottom) at  $\mu = 0$  and  $Tl^{2/3} = 1$  around  $x = l$  where  $\mu_{\text{eff}} = 1$ .

fore, the leading  $T = 0$  scaling behavior (35) associated with the exponent  $2p/(p+1)$  is also effectively averaged out by the temperature.

#### IV. TSS AROUND THE SPATIAL POINT WHERE $\mu_{\text{eff}}(x) = 1$

When  $\mu < 1$ , the region where the particle density appears to rapidly vanish corresponds to the region where the effective chemical potential defined in Eq. (21) approaches the values  $\mu_{\text{eff}} \approx 1$ , which is the value of the chemical potential corresponding to the transition be-

tween the superfluid phase and the empty state, where the particle density of the ground state gets suppressed. We thus expect that, for generic values of  $\mu$  and  $p$ , the region around

$$x_c = l(1 - \mu)^{1/p}, \quad (36)$$

where  $\mu_{\text{eff}}(x_c) = 1$ , develops critical modes related to the superfluid to vacuum transition. The effective chemical potential can be expanded around  $x_c$  as

$$\mu_{\text{eff}}(x) = 1 + p(1 - \mu)^{(p-1)/p} \frac{x - x_c}{l} + O[(x - x_c)^2]. \quad (37)$$

Therefore the behavior around  $x_c$  is essentially analogous to that arising at  $\mu = 1$  in the presence of a linear potential  $V_l \sim r/l$ . Around  $x_c$ , critical modes should appear with length scale  $\xi \sim l^\sigma$ , where  $\sigma$  is the exponent associated with a linear external potential, thus [25]  $\sigma = 1/3$ , obtained by replacing  $p = 1$  in Eq. (5). We then expect that around  $x = x_c$

$$\rho(x) = l^{-1/3} f_\rho[(x - x_c)/l^{1/3}, Tl^{2/3}], \quad (38)$$

$$\Delta\rho(x) \equiv \rho - \rho_{\text{da}} = l^{-1/3} f_{\Delta\rho}[(x - x_c)/l^{1/3}, Tl^{2/3}], \quad (39)$$

$$G(x_c, x) = l^{-2/3} f_g[(x - x_c)/l^{1/3}, Tl^{2/3}]. \quad (40)$$

In Fig. 10 we show QMC results at  $\mu = 0$  for some values of  $l$  keeping  $Tl^{2/3} = 1$  fixed, which nicely confirm the scaling behaviors (38-40). Note that analogous results are obtained for any  $\mu < 1$ , around the region where  $\mu_{\text{eff}}(x) \approx 1$ .

## V. CONCLUSIONS

We have investigated the interplay of temperature and trap effects in cold particle systems at their quantum critical regime, such as cold bosonic atoms in optical lattices at the transitions between Mott-insulator and superfluid phases. The theoretical framework is provided by the 1D Bose-Hubbard model (1) in the presence of an external trapping potential, and by the TSS theory leading to the TSS ansatz (4) and (7). This study is of experimental relevance, because quasi 1D trapped particle systems have been realized in optical lattices, see, e.g., Refs. [1, 4, 5, 9]. Therefore, temperature and trap effects at the Mott transitions may be investigated by improving the accuracy of the experiments.

Our numerical study is based on QMC simulations at fixed chemical potential and trap size. Since the main features of the TSS at the Mott transitions are expected to be universal with respect to the on-site coupling  $U$  (provided  $U > 0$ ), we consider the HC limit  $U \rightarrow \infty$ , which is particularly convenient because it restricts the values of the site particle number to  $n_x = 0, 1$ , and it is expected to minimize the corrections to the universal TSS, as verified at  $T = 0$  [30]. We present finite-temperature results for the particle density and the

density-density correlator, at the quantum Mott transitions, and within the gapless superfluid phase. Their temperature and trap-size dependences appear well described by the simplest TSS ansatz, such as that given in Eq. (7) with  $\theta = p/(p + 2)$ . In particular, the finite-temperature data do not show evidence of the periodic modulations of the asymptotic behaviors which are observed at  $T = 0$  [25]. They are effectively averaged out by a nonzero temperature, leaving only a plain power-law TSS behavior.

## Acknowledgments

The QMC simulations were performed at the INFN Pisa GRID DATA center, using also the cluster CSN4.

## Appendix A: The QMC simulations

Our numerical study of the BH model (1) is based on QMC simulations using the stochastic series expansion method [27] with the directed loop algorithm [28]. We compute the particle density  $\langle n_x \rangle$  and its connected correlation function  $\langle n_x n_y \rangle_c$ .

The QMC simulations are performed at fixed temperature  $T$ , chemical potential  $\mu$ , trap size  $l$ , and lattice size  $L$  with open boundary conditions. In order to avoid finite-size effects, we choose  $L$  sufficiently large to effectively obtain  $L \rightarrow \infty$  data within the statistical errors.

QMC simulations require also to fix some algorithm parameters, such as the order  $N_{\text{tr}}$  of the truncation of the Taylor expansion of the partition function, and the number of operator loops  $N_{\text{loops}}$ . We set  $N_{\text{tr}}$  in the standard way as  $N_{\text{tr}} = 1.5 M_{\text{max}} N_{\text{bonds}}/T$  where  $M_{\text{max}}$  is the highest matrix element of the single bond Hamiltonians and  $N_{\text{bonds}}$  is the number of interacting site pairs. At the end of each simulation we analyze the fluctuation in the order of the series expansion, and verify whether the averaged order is safely less than  $N_{\text{tr}}$ , and its deviations have the expected behavior proportional to the square root of the mean value. We define a MC step as a single sweep of identity and diagonal operators in the expansion of the partition function followed by a number  $N_{\text{loops}}$  of directed operator loop updates. The number  $N_{\text{loops}}$  is fixed by requiring that the number of visited vertices is globally of the order of  $N_{\text{tr}}$  in a MC step.

Typical statistics of our QMC simulations are a few million MC steps for each set of parameters. We have checked that, in all QMC simulations presented here, the autocorrelation times of the observables that we compute are smaller than  $10^2$  in units of MC steps. Effective  $L \rightarrow \infty$  data within the resulting statistical errors are obtained by taking  $L/l \approx 4$  for the simulations at  $\mu = 1$  and  $\mu = 0$ , and  $L/l \approx 9$  for  $\mu = -1$ .

Let us now discuss the operator-loop equations. Since the Hamiltonian of the HC BH model can be written

as a sum of bond terms, and since there is a one-to-one correspondence between the site occupation number and the states of the XXZ model [29], the non-zero matrix elements are the same as those reported in Ref. [28] (see its Sec. 2). Of course, their values are different, in particular the diagonal matrix elements are site dependent, due to the existence of the trap which gives rise to a space-dependent effective chemical potential  $\mu_{\text{eff}}(x)$ . Using considerations based on the symmetry and conservation laws, we can divide the transition probabilities

involved in the operator-loop update in eight independent groups for each site, as in Ref. [28] (see its Sec. 3), with three possible bounces (probabilities to exit the actual visited vertex of the operator loop from the same entrance leg) for each group. The corresponding system of equations are solved by minimizing the bounces. As a result, we allow one bounce within each group in the QMC simulations at  $\mu = 1$  and  $\mu = 0$ , and two bounces at  $\mu = -1$ .

- 
- [1] I. Bloch, J. Dalibard, and W. Zwerger, *Rev. Mod. Phys.* 80, 885 (2008).
- [2] M. Greiner, I. Bloch, M.O. Mandell, T. Hänsch, and T. Esslinger, *Nature* 415, 39 (2002).
- [3] T. Stöferle, H. Moritz, C. Schori, M. Köhl, and T. Esslinger, *Phys. Rev. Lett.* 92, 130403 (2004).
- [4] B. Paredes, A. Widera, V. Murg, O. Mandel, S. Fölling, I. Cirac, G. Shlyapnikov, R.W. Hänsch, and I. Bloch, *Nature* 429, 277 (2004).
- [5] T. Kinoshita, T. Wenger, and D.S. Weiss, *Science* 305, 1125 (2004); *Phys. Rev. Lett.* 95, 190406 (2005).
- [6] Z. Hadzibabic, P. Krüger, M. Cheneau, B. Battelier, and J. Dalibard, *Nature* 441, 1118 (2006).
- [7] S. Fölling, A. Widera, T. Müller, F. Gerbier, and I. Bloch, *Phys. Rev. Lett.* 97, 060403 (2006).
- [8] I.B. Spielman, W.D. Phillips, and J.V. Porto, *Phys. Rev. Lett.* 98, 080404 (2007); *Phys. Rev. Lett.* 100, 120402 (2008).
- [9] D. Clément, N. Fabbri, L. Fallani, C. Fort, and M. Inguscio, *Phys. Rev. Lett.* 102, 155301 (2009).
- [10] D. Jaksch, C. Bruder, J.I. Cirac, C.W. Gardiner, and P. Zoller, *Phys. Rev. Lett.* 81, 3108 (1998).
- [11] M.P.A. Fisher, P.B. Weichmann, G. Grinstein, and D.S. Fisher, *Phys. Rev. B* 40, 546 (1989).
- [12] In two dimensions logarithmic corrections may arise due to the fact that  $d = 2$  is the upper critical space dimension of the corresponding continuum theory.
- [13] G.G. Batrouni, V. Rousseau, R.T. Scalettar, M. Rigol, A. Muramatsu, P.J.H. Denteneer, and M. Troyer, *Phys. Rev. Lett.* 89, 117203 (2002).
- [14] V.A. Kashurnikov, N.V. Prokofev, and B.V. Svistunov, *Phys. Rev. A* 66, 031601 (2002).
- [15] C. Kollath, U. Schollwöck, J. von Delft, W. Zwerger, *Phys. Rev. A* 69, 031601 (2004).
- [16] L. Pollet, S. Rombouts, K. Heyde, and J. Dukelsky, *Phys. Rev. A* 69, 043601 (2004).
- [17] S. Wessel, F. Alet, M. Troyer, and G.G. Batrouni, *Phys. Rev. A* 70, 053615 (2004).
- [18] M. Rigol and A. Muramatsu, *Phys. Rev. A* 70, 031603 (2004); *Phys. Rev. A* 72, 013604 (2005).
- [19] B. DeMarco, C. Lannert, S. Vishveshwara, and T.-C. Wei, *Phys. Rev. A* 71, 063601 (2005).
- [20] O. Gygi, H.G. Katzgraber, M. Troyer, S. Wessel, and G.G. Batrouni, *Phys. Rev. A* 73, 063606 (2006).
- [21] L. Urba, E. Lundh, and A. Rosengren, *J. Phys. B* 39, 5187 (2006).
- [22] M. Rigol, G.G. Batrouni, V.G. Rousseau and R.T. Scalettar, *Phys. Rev. A* 79, 053605 (2009).
- [23] M. Campostrini and E. Vicari, *Phys. Rev. A* 81, 023606 (2010).
- [24] M. Campostrini and E. Vicari, *Phys. Rev. Lett.* 102, 240601 (2009).
- [25] M. Campostrini and E. Vicari, *Phys. Rev. A* 81, 063614 (2010).
- [26] S.L.A. de Queiroz, R.R. dos Santos, and R.B. Stinchcombe, *Phys. Rev. E* 81, 051122 (2010).
- [27] A.W. Sandvik, *Phys. Rev. B* 59, R14157 (1999).
- [28] O.F. Syljuasen and A.W. Sandvik, *Phys. Rev. E* 66, 046701 (2002).
- [29] In the HC limit the 1D BH model can be mapped into the XX chain model with a space-dependent transverse external field,  $H_{\text{XX}} = -J \sum_i (S_i^x S_{i+1}^x + S_i^y S_{i+1}^y) + \sum_i [\mu + V(x_i)] S_i^z$ , where  $S_i^a = \sigma_i^a / 2$  and  $\sigma^a$  are the Pauli matrices, which are related to the boson operators  $b_i$  by  $\sigma_i^x = b_i^\dagger + b_i$ ,  $\sigma_i^y = i(b_i^\dagger - b_i)$ ,  $\sigma_i^z = 1 - 2b_i^\dagger b_i$ . Then, by a Jordan-Wigner transformation, one can further map it into a model of spinless fermions, see, e.g., Ref. [31].
- [30] M. Campostrini and E. Vicari, *Phys. Rev. A* 82, 063636 (2010).
- [31] S. Sachdev, *Quantum Phase Transitions* (Cambridge Univ. Press, 1999).
- [32] M. Campostrini and E. Vicari, *J. Stat. Mech.: Theory Exp.* (2010) P08020.